

Regularized Adaptive Long Autoregressive Spectral Analysis

Jean-François Giovannelli, Jérôme Idier, Daniel Muller, and Guy Desodt

© 2001 IEEE. Personal use of this material is permitted. However, permission to reprint/republish this material for advertising or promotional purposes or for creating new collective works for resale or redistribution to servers or lists, or to reuse any copyrighted component of this work in other works must be obtained from the IEEE.

Abstract—This paper is devoted to adaptive long autoregressive spectral analysis when i) very few data are available and ii) information does exist beforehand concerning the spectral smoothness and time continuity of the analyzed signals. The contribution is founded on two papers by Kitagawa and Gersch [1], [2]. The first one deals with spectral smoothness in the regularization framework, while the second one is devoted to time continuity in the Kalman formalism. The present paper proposes an original synthesis of the two contributions. A new regularized criterion is introduced that takes both pieces of information into account. The criterion is efficiently optimized by a Kalman smoother. One of the major features of the method is that it is entirely unsupervised. The problem of automatically adjusting the hyperparameters that balance data-based versus prior-based information is solved by maximum likelihood (ML). The improvement is quantified in the field of meteorological radar.

Index Terms—Adaptive spectral analysis, hyperparameter estimation, long autoregressive model, maximum likelihood (ML), meteorological Doppler radar, regularization, spectral smoothness, time continuity.

I. INTRODUCTION

ADAPTIVE spectral analysis and time-frequency analysis are of major importance in fields as widely varied as speech processing [3], acoustical attenuation measurements [4], [5], ultrasonic Doppler velocimetry [6], or Doppler radars [7]–[11]. [12] gives a synthesis of the various methods for these problems, and provides a number of bibliographical introductions.

The present paper focuses on short-time analysis. Typically, for analysis of pulsed Doppler signals, only eight or 16 samples are available to estimate one spectrum, with possibly various shapes (multimodal or not, of large spectral width or not, mixed clutter, etc.). Under such circumstances, the construction of the sought spectra becomes extremely tricky on the sole basis of the samples. As a point of reference, let us recall that several hundred samples are usually needed to compute an averaged periodogram with a fair bias-variance compromise [13], [14]. Therefore, parametric methods have generally been preferred, among which autoregressive (AR) methods play a central role. The AR coefficients estimation is usually tackled in the least squares (LS) framework [15], [16]. These methods often provide a solution at points where nonparametric methods are

useless. But when the number of data is very low, these techniques become, in their turn, useless, especially if various spectral shapes are expected due to model order limitations.

In order to construct a reliable image, structural information about the sought spectrum sequence must be accounted for. Our investigation is therefore restricted to the cases in which two kinds of information are foreknown: *spectral smoothness* and *time continuity*. This *a priori* information is the foundation of the proposed construction.

In the framework of stationary AR analysis, Kitagawa and Gersch proposed a method integrating the idea of spectral smoothness [1] by which a *high-order AR model* can be robustly estimated, thereby getting around the difficult problem of order selection and providing the ability to estimate various spectral shapes. For the nonstationary case, and aside from [1], the same authors introduced in [2] a Markovian model for the regressor sequence in the Kalman formalism in order to reflect time continuity. The present paper reviews [1] and [2] and makes an original synthesis suited to the special configuration of Doppler signals. A new Regularized LS (RegLS) criterion simultaneously includes the spectral and time information and is optimized by a Kalman smoother (KS).

One of the major features of the method is that it is entirely unsupervised: the adjustment of parameters that weight the relative contributions of the observation *versus* the *a priori* knowledge is automatically set by maximum likelihood (ML).

A comparative study is proposed in the context of pulsed Doppler radars. Special attention is paid to atmospheric and/or meteorological context imaging or identification: ground clutter, rain clutter, sea echos, etc. Adaptive spectral estimation of mixed clutter is achieved by means of several usual AR methods and the proposed one. The latter achieves qualitative and quantitative improvements w.r.t. usual methods.

The paper is organized as follows. Section II mainly introduces notations and problem statement. Section III focuses on usual LS methods and usual adaptive extensions. The proposed method is presented in Section IV, and Section V deals with the KS. The problem of automatic parameter estimation is addressed in Section VI. Simulation results are presented in Section VII. Finally, conclusions and perspectives for future works are presented in Section VIII.

II. PROBLEM STATEMENT

The problem is that of processing pulsed Doppler signals from electronic scanning radars or ultrasound velocimeter. The reader may consult [6], [7] for a technological review. The pulsed Doppler systems are such that the observed signals do

Manuscript received May 31, 20; revised January 19, 2001.

J.-F. Giovannelli and J. Idier are with the Laboratoire des Signaux et Systèmes (CNRS-SIPÉLEC-UPS) SUPÉLEC, 91192 Gif-sur-Yvette Cedex, France (e-mail: giova@lss.supelec.fr; idier@lss.supelec.fr).

D. Muller and G. Desodt are with the Société Thomson, 92220 Bagneux, France.

Publisher Item Identifier S 0196-2892(01)09291-9.

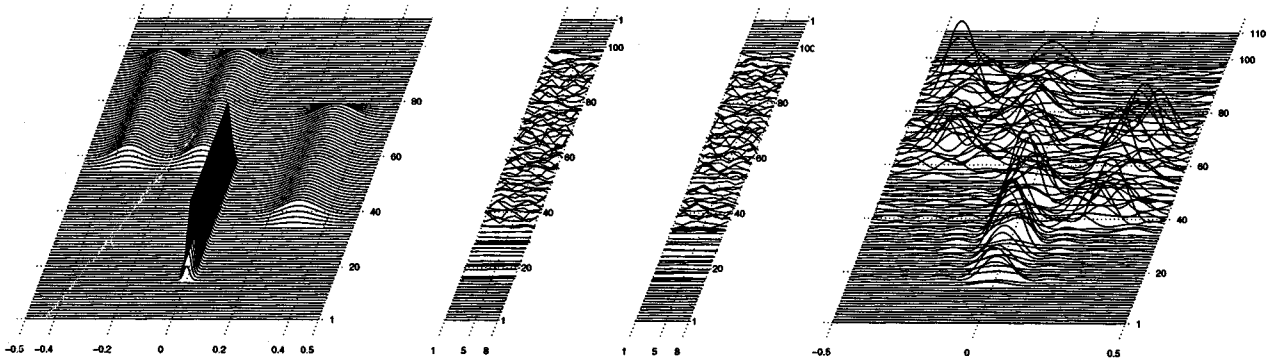


Fig. 1. Simulated observations over 110 range bins with eight samples per bin (corresponding to eight Doppler pulses). The left-hand side (LHS) figure shows the true spectra sequence. The narrow zero-mean spectra characterizes ground clutter (bin 15 to 57). Rain clutter induces more or less broad, single-mode spectra (bin 35 to 75). Lastly, sea echos resulting from wave phenomena exhibit two maxima (bin 56 to 95). The middle figure shows the real part and imaginary part of the data and the rhs one shows the associated periodograms.

not occur in the usual form of time-frequency problems. So, neither the usual time-frequency methods nor the one proposed by Kitagawa and Gersch can be directly applied, and part of the presented work consists in constructing an appropriate method for the encountered configuration.

The measurements are available as a set of complex signals $\mathcal{Y} = [\mathbf{y}_1, \dots, \mathbf{y}_M]$, depth-wise juxtaposed in M range bins. It is assumed that each $\mathbf{y}_m = [y_{m1}, \dots, y_{mN}]^t$ is a N sample vector extracted from a zero-mean stationary process. Fig. 1 gives a Gaussian simulated example over $M = 110$ bins for which $N = 8$ samples are observed per bin. The successive regressors are denoted $\mathbf{a}_m = [a_{mp}]$, where m indicates the considered bin ($m \in \mathbb{N}_M^* = \{1, 2, \dots, M\}$) and p the order of the autoregression coefficient ($p \in \mathbb{N}_P^*$). Let us note $\mathbf{A} = [\mathbf{a}_1, \dots, \mathbf{a}_M] \in \mathbb{C}^{N \times P}$ the collection of the whole set of coefficients. Let us also introduce r_m and r_m^e for signal and prediction error powers. The remainder of the paper is devoted to estimation of these quantities. The next section deals with the usual LS methods and their adaptive extension, and shows their inadequacy for the problem at stake.

III. REVIEW OF CLASSICAL METHODS

A. Stationary Spectral Analysis

This subsection is devoted to spectral analysis applied to a single bin m . Assuming a Gaussian distribution for the observed signal, the likelihood of the AR coefficients $f(\mathbf{y}_m | \mathbf{a}_m)$ shows a special form [17, p. 82], but its maximization raises a difficult problem. A few authors [18], [19] have undertaken to solve it, but firstly, the available algorithms cannot guarantee global maximization, and secondly, they are not computationally efficient for the applications under the scope of the paper. To remedy these disadvantages, the following approximation of the likelihood function is usually accepted [16, p. 185]:

$$f(\mathbf{y}_m | \mathbf{a}_m) = (\pi r_m^e)^{-N} \exp\left(\frac{-Q_m^{\text{LS}}(\mathbf{a}_m)}{r_m^e}\right) \quad (1)$$

involving the norm of the prediction error vector

$$Q_m^{\text{LS}}(\mathbf{a}_m) = \mathbf{e}_m^\dagger \mathbf{e}_m = (\mathbf{y}_m - Y_m \mathbf{a}_m)^\dagger (\mathbf{y}_m - Y_m \mathbf{a}_m) \quad (2)$$

i.e., a quadratic form with regard to the \mathbf{a}_m , namely, the LS criterion. The \mathbf{y}_m and Y_m are the vector and matrix designed according to some chosen windowing assumption [15, p. 217], [20, (2)]. There are four possible forms: nonwindowed (covariance method), prewindowed, postwindowed, double-windowed, i.e., pre- and postwindowed (autocorrelation method). Let us note L , the size of \mathbf{y}_m : $L = N - P$, $L = N$, or $L = N + P$, according to the chosen form. This choice is of importance since it strongly influences spectral resolution for short time analysis [15].

Whatever the chosen form, the maximization of (1) comes down to the minimization of (2) and yields

$$\hat{\mathbf{a}}_m^{\text{LS}} = \arg \min_{\mathbf{a}_m} Q_m^{\text{LS}}(\mathbf{a}_m) = (Y_m^\dagger Y_m)^{-1} Y_m^\dagger \mathbf{y}_m. \quad (3)$$

As a prerequisite, the problem of choosing the model order P must be tackled. P must be high enough to describe various PSD and low enough to avoid spurious peaks, i.e., to ensure spectral smoothness. This compromise can usually be set by means of criteria such as FPE [21], AIC [22], CAT [23], or MDL [24], but, in the situation of prime interest here, they fail because the available amount of data is too small [25]. Actually, there exists no satisfying compromise in term of model order, since too few data are available to estimate DSPs with possibly complex structures.

B. Adaptive Spectral Analysis

For the “multirange bin” analysis, the first idea consists in processing each bin independently. According to the LS approach, it amounts to minimizing a global LS criterion

$$Q^{\text{LS}}(\mathbf{A}) = \sum_{m=1}^M Q_m^{\text{LS}}(\mathbf{a}_m). \quad (4)$$

However, the resulting spectra hold unrealistic variations in the spatial direction (see Fig. 4). In order to remedy this problem, the adaptive least squares (ALS) approach accounts for spatial continuity by processing the data from several bins, possibly in weighted form, to estimate each \mathbf{a}_m . A first approach uses a series of LS criteria including the data in a spatial window of length W . A widely used alternative is the exponential decay

memory which uses geometrically weighted LS criteria, with parameter $\lambda \in [0, 1]$. The latter is more popular because it is simpler: λ is merely incorporated into a standard recursive LS algorithm [15, p. 266]. In both cases, the degree of adaptivity, i.e., the spatial continuity is modulated by W or λ .

C. Conclusion

Whatever the variant, the main disadvantage of these approaches has to do with the parameter settings.

- 1) From the spectral standpoint, smoothness is introduced in a roundabout fashion, *via* the model order (adjusted by P) and the compromise no longer exists when the amount of data is reduced.
- 2) From the spatial standpoint, continuity is also indirectly introduced (and tuned by W or λ) and no automatic method for adjusting this parameters is available.

These limitations are unavoidable in the simple LS formalism, and to alleviate this problem, we resort to the regularization theory. In this framework, the proposed approach:

- includes the spectral smoothness and spatial continuity in the estimation criterion itself;
- allows long-AR model to be robustly estimated, and then various spectra to be identified;
- provides automatic parameter setting, i.e., an entirely unsupervised method.

IV. LONG AR (SPATIAL CONTINUITY) SPECTRAL SMOOTHNESS

A. Spatial Continuity Model

The first idea consists in building a spectral distance. Following [2], starting with the PSD in bin m

$$S_m(\nu) = \frac{r_m^e}{|1 - A_m(\nu)|^2}, \quad A_m(\nu) = \sum_{p=1}^P a_{mp} e^{-2j\pi\nu p} \quad (5)$$

the proposed spectral distance between S_m and $S_{m'}$ is founded on the k th Sobolev distance between A_m and $A_{m'}$

$$D_k(m, m') \propto \int_0^1 \left| \frac{d^k}{d\nu^k} [A_m(\nu) - A_{m'}(\nu)] \right|^2 d\nu.$$

Calculations similar to those of [2] yield a quadratic form

$$D_k(m, m') = (\mathbf{a}_m - \mathbf{a}_{m'})^\dagger \Delta_k (\mathbf{a}_m - \mathbf{a}_{m'}) \quad (6)$$

where $\Delta_k = \text{diag}[1^{2k}, \dots, P^{2k}]$ is the k th spectral matrix.

B. Spectral Smoothness Model

The spectral smoothness measure proposed by Kitagawa and Gersch in [2] (see also [26]) is easily deduced from (6) as the distance to a constant DSP

$$D_k(m) \propto \mathbf{a}_m^\dagger \Delta_k \mathbf{a}_m. \quad (7)$$

According to [1], [2], $k \in \mathbb{Z}_+$, but Δ_k as well as (6) and (7) can be extended to $k \in \mathbb{R}_+$.

Remark 1: Strictly speaking, $D_k(m, m')$ and $D_k(m)$ are not spectral distances nor spectral smoothness measures since they are not functions of the PSD itself. However, they are quadratic and this has two advantages: it considerably simplifies regressor

calculations (see Section V) as well as regularization parameter estimation (see Section VI).

C. Double Smoothness

Starting with the spectral smoothness (7) and the spatial distance (6), a new quadratic penalization is introduced

$$Q^\infty(\mathbf{A}) = \frac{1}{r_s} \sum_{m=1}^M D_k(m) + \frac{1}{r_d} \sum_{m=1}^{M-1} D_k(m, m+1). \quad (8)$$

It integrates both spectral smoothness and spatial continuity, respectively, tuned by $\lambda_s = 1/r_s$ and $\lambda_d = 1/r_d$.

Remark 2: The penalization (8) has a Bayesian interpretation [27] as a Gaussian prior for the sought regressors

$$f(\mathbf{A}) \propto \exp[-Q^\infty(\mathbf{A})] \quad (9)$$

useful for hyperparameter estimation in Section VI.

D. Regularized Least Squares

From the LS criteria (4) and the penalization term (8), the proposed RegLS criterion reads

$$\begin{aligned} Q^{\text{Reg}}(\mathbf{A}) &= Q^{\text{LS}}(\mathbf{A}) + Q^\infty(\mathbf{A}) \\ &= \sum_{m=1}^M \frac{1}{r_m^e} (\mathbf{y}_m - Y_m \mathbf{a}_m)^\dagger (\mathbf{y}_m - Y_m \mathbf{a}_m) \\ &\quad + \frac{1}{r_s} \sum_{m=1}^M \mathbf{a}_m^\dagger \Delta_k \mathbf{a}_m \\ &\quad + \frac{1}{r_d} \sum_{m=1}^{M-1} (\mathbf{a}_m - \mathbf{a}_{m+1})^\dagger \Delta_k (\mathbf{a}_m - \mathbf{a}_{m+1}) \end{aligned} \quad (10)$$

involving three terms which respectively measure fidelity to the data, spectral smoothness and spatial regularity. The regularized solution is defined as the minimizer of (10)

$$\hat{\mathbf{A}}_{\text{Reg}} = \arg \min_{\mathbf{A}} Q^{\text{Reg}}(\mathbf{A}). \quad (11)$$

Remark 3: The regularized criterion (10) has a clear Bayesian interpretation [27]. Likelihood (1) and prior (9) can be fused thanks to the Bayes rule, into a Gaussian posterior law for the sought regressors

$$f(\mathbf{A}|\mathcal{Y}) \propto \exp[-Q^{\text{Reg}}(\mathbf{A})]. \quad (12)$$

Solution (11) is also the MAP estimate.

E. Optimization Stage

Several options are available to compute (11). Since $Q^{\text{Reg}}(\mathbf{A})$ is quadratic, $\hat{\mathbf{A}}_{\text{Reg}}$ is the solution of an $MP \times MP$ linear system. Moreover, since the involved matrix is sparse, direct inversion should be tractable but not recommendable here ($M = 110$, $P = 7$). Another approach may be found in gradient or relaxation methods [28] since $Q^{\text{Reg}}(\mathbf{A})$ is differentiable and convex. But, given the depth-wise structure, another algorithm is preferred: KS. Here we resort to the initial viewpoint of Kitagawa and Gersch in [2]. However, it is

noticeable that [2] does not mention the minimized criterion, whereas our KS is designed to minimize (10).

V. KALMAN SMOOTHING

A. State-Space Form

- 1) The successive prediction vectors \mathbf{a}_m are related by a first-order state equation

$$\mathbf{a}_{m+1} = \alpha_m \mathbf{a}_m + \varepsilon_m \quad (13)$$

in which each ε_m is a complex, zero-mean, circular, vector with covariance matrix $P_m^\varepsilon = r_m^\varepsilon \Delta_k^{-1}$ and the ε_m -sequence, is depth-wise white.

- 2) The full state model also brings in the initial mean and covariance: the null vector and $P^a = r^a \Delta_k^{-1}$, respectively.
- 3) The observation equation is the recurrence equation for the AR model in each bin, written in compact form as

$$\mathbf{y}_m = Y_m \mathbf{a}_m + \mathbf{e}_m \quad (14)$$

i.e., a generalized version of the one proposed in [2], adapted to depthwise vectorial data. Each \mathbf{e}_m is a complex, zero-mean, circular vector with covariance $r_m^\varepsilon I_L$. The \mathbf{e}_m sequence is also depthwise white.

Remark 4: [2] accounts for spatial continuity by means of a special case of (13): $\mathbf{a}_{m+1} = \mathbf{a}_m + \varepsilon_m$. The latter has two drawbacks, though. Firstly, it is introduced apart from the idea of spectral smoothness. Secondly, from a Bayesian point of view, this equation is interpreted as a Brownian process with an increasing variance, which may cause drifts to appear in the estimated spectra. On the contrary, the new coefficients α_m can be chosen in order to ensure stationarity of the model (13) or to minimize the homogeneous criterion (10).

B. Equivalence Between Parameter Settings

1) *Homogeneous Criterion:* This section establishes the formal link between the parameters of the KS (r^a and $\alpha_m, r_m^\varepsilon$) and those of the regularized criterion (10) (r_d and r_s). [29] states that the KS associated to (13) and (14) minimizes $Q^{\text{KS}}(\mathbf{A})$

$$\begin{aligned} &= \sum_{m=1}^M \frac{1}{r_m^\varepsilon} (\mathbf{y}_m - Y_m \mathbf{a}_m)^\dagger (\mathbf{y}_m - Y_m \mathbf{a}_m) \\ &+ \sum_{m=1}^{M-1} \frac{1}{r_m^\varepsilon} (\mathbf{a}_{m+1} - \alpha_m \mathbf{a}_m)^\dagger \Delta_k^{-1} (\mathbf{a}_{m+1} - \alpha_m \mathbf{a}_m) \\ &+ \frac{1}{r^a} \mathbf{a}_1^\dagger \Delta_k^{-1} \mathbf{a}_1. \end{aligned} \quad (15)$$

Partial expansions yield identification of (10) and (15) through the following count-down recursion.

- 1) Initialization ($m = M - 1$)

$$\alpha_{M-1} = (1 + \rho)^{-1}, \quad \text{and } r_{M-1}^\varepsilon = r_d \alpha_{M-1}.$$

- 2) Count-down recursion ($m = M - 2, \dots, 1$)

$$\alpha_m = (2 + \rho - \alpha_{m+1})^{-1}, \quad \text{and } r_m^\varepsilon = r_d \alpha_m.$$

- 3) The last step yields the initial power

$$r^a = r_d (1 + \rho - \alpha_1)^{-1}$$

with $\rho = r_d / r_s \in \mathbb{R}_+^*$. These equations allow us to pre-compute the coefficients of the KS in order to minimize (10).

2) *Limit Model:* This section is devoted to the asymptotic behavior of the α_m -sequence. For the sake of notational simplicity, the sequence is rewritten in a count-up form

$$\begin{aligned} m=1: \bar{\alpha}_1 &= (1 + \rho)^{-1} \\ m \in \mathbb{N}^*: \tilde{\alpha}_{m+1} &= (2 + \rho - \bar{\alpha}_m)^{-1}. \end{aligned} \quad (16)$$

It is clear that $\tilde{\alpha}_1 \in]0, 1[$ since $\rho \in \mathbb{R}_+^*$. Let us introduce $f(u) = (2 + \rho - u)^{-1}$. It is straightforward that $f(]0, 1[) \subset]0, 1[$, so the entire $\tilde{\alpha}_m$ -sequence remains in $]0, 1[$. Moreover, if it exists, the limit $\alpha_\infty \in [0, 1]$ necessarily fulfills $f(\alpha_\infty) = \alpha_\infty$. Elementary algebra yields

$$\alpha_\infty = \frac{\theta - \sqrt{\theta^2 - 4}}{2} \quad (17)$$

with $\theta = 2 + \rho = 2 + r_d / r_s$. Finally, one can effortlessly see that $\forall u, v \in]0, 1[$, we have $|f(u) - f(v)| \leq (1 + \rho)^{-2} |u - v|$, i.e., f is a Lipschitz function with ratio in $]0, 1[$. Hence, the sequence effectively converges toward α_∞ . It is also easy to see that the sequence is monotonous: increasing if $\alpha_1 < \alpha_\infty$ and decreasing otherwise. In the present case, comparison of α_1 in (16) and α_∞ in (17) shows that the $\tilde{\alpha}_m$ -sequence is decreasing (in the count-up form), hence, α_m is increasing.

Finally, since $r_m^\varepsilon = r_d \alpha_m$, the corresponding limit state power is given by

$$r_\infty^\varepsilon = r_d \alpha_\infty. \quad (18)$$

3) *Associated Stationary Criterion:* This section is devoted to the stationary limit model: the special case of (13), with $\alpha_m = \alpha_\infty$ and $r_m^\varepsilon = r_\infty^\varepsilon$, i.e., a stationary first-order AR model for the \mathbf{a}_m -sequence. The initial power is denoted r_∞^a for notational coherence, even if it is not defined as a limit. It is actually defined according to r_∞^ε and α_∞ in order to ensure stationarity for the first-order AR model: $r_\infty^a = r_\infty^\varepsilon / (1 - \alpha_\infty^2)$.

Replacement of $\alpha_m, r_m^\varepsilon, r^a$ by $\alpha_\infty, r_\infty^\varepsilon, r_\infty^a$ in (15) yields the criterion minimized by the stationary KS

$$\begin{aligned} Q^{\text{S}}(\mathbf{A}) &= \sum_{m=1}^M \frac{1}{r_m^\varepsilon} (\mathbf{y}_m - Y_m \mathbf{a}_m)^\dagger (\mathbf{y}_m - Y_m \mathbf{a}_m) \\ &+ \frac{(1 - \alpha_\infty)^2}{r_\infty^\varepsilon} \sum_{m=1}^M \mathbf{a}_m^\dagger \Delta_k \mathbf{a}_m \\ &+ \frac{\alpha_\infty}{r_\infty^\varepsilon} \sum_{m=1}^{M-1} (\mathbf{a}_m - \mathbf{a}_{m+1})^\dagger \Delta_k (\mathbf{a}_m - \mathbf{a}_{m+1}) \\ &+ \frac{\alpha_\infty (1 - \alpha_\infty)}{r_\infty^\varepsilon} \left(\mathbf{a}_1^\dagger \Delta_k \mathbf{a}_1 + \mathbf{a}_M^\dagger \Delta_k \mathbf{a}_M \right) \end{aligned}$$

where superscript “S” stands for stationary. Since we have $r_d = r_\infty^\varepsilon/\alpha_\infty$ from (18) and $r_s = r_\infty^\varepsilon/(1 - \alpha_\infty)^2$ from (17), one can effortlessly see that

$$Q^S(\mathbf{A}) = Q^{\text{Reg}}(\mathbf{A}) + \frac{\alpha_\infty(1 - \alpha_\infty)}{r_\infty^\varepsilon} \left(\mathbf{a}_1^\dagger \Delta_k \mathbf{a}_1 + \mathbf{a}_M^\dagger \Delta_k \mathbf{a}_M \right).$$

So the stationary criterion $Q^S(\mathbf{A})$ and the initial homogeneous one $Q^{\text{Reg}}(\mathbf{A})$ are equal apart from the edge effects, i.e., two terms regarding the first and last regressors. As a consequence, the minimizer of $Q^{\text{Reg}}(\mathbf{A})$ and $Q^S(\mathbf{A})$ are practically equivalent and the latter is preferred since it does not require precomputation of the α_m and r_m^ε .

C. Kalman Smoother Equations

- Initialization ($m = 1$)

$$\mathbf{a}_{1|1} = 0 \quad (19)$$

$$P_{1|1} = r_\infty^\varepsilon \Delta_k^{-1}. \quad (20)$$

- Filtering phase (for $m = 2, \dots, M$)
 - Prediction step

$$\mathbf{a}_{m|m-1} = \alpha_\infty \mathbf{a}_{m-1|m-1} \quad (21)$$

$$P_{m|m-1} = \alpha_\infty^2 P_{m-1|m-1} + r_\infty^\varepsilon \Delta_k^{-1}. \quad (22)$$

- Correction step

$$K_m = P_{m|m-1} Y_m^\dagger \quad (23)$$

$$R_m = r_m^\varepsilon I_L + K_m^\dagger Y_m \quad (24)$$

$$\mathbf{e}_m = \mathbf{y}_m - Y_m \mathbf{a}_{m|m-1} \quad (25)$$

$$\mathbf{a}_{m|m} = \mathbf{a}_{m|m-1} + K_m R_m^{-1} \mathbf{e}_m. \quad (26)$$

$$P_{m|m} = P_{m|m-1} - K_m R_m^{-1} K_m^\dagger. \quad (27)$$

- Smoothing count-down phase (for $m = M - 1, \dots, 1$)

$$Q_m = \alpha_\infty P_{m|m} P_{m+1|m}^{-1} \quad (28)$$

$$\mathbf{a}_{m|M} = \mathbf{a}_{m|m} + Q_m (\mathbf{a}_{m+1|M} - \mathbf{a}_{m+1|m}) \quad (29)$$

$$P_{m|M} = P_{m|m} + Q_m (P_{m+1|M} - P_{m+1|m}) Q_m^\dagger. \quad (30)$$

D. Fast Algorithm

Fast algorithms used to take a primordial position in past decades, especially for real-time computations. More specifically, for adaptive spectral analysis of the ultrasound Doppler signal, the MARASCA algorithm [27] has been used in a real-time high-resolution velocimeter prototype. But it has two drawbacks, resulting in a rigid spectral and spatial continuity tuning. On the one hand, it proceeds by blocks and incorporates spatial continuity by using the regressor of the current block as a prior mean for the next one; on the other hand, the fast version is developed only for the zero-order smoothness ($k = 0$).

To our knowledge, no fast algorithm exists for the KF in the configuration of interest, mainly because of the structures of the

state equation and the smoothness matrix. However, a fast algorithm may be developed on the basis of high-order displacement matrices [30]. More precisely, it is easy to see that the displacement matrix of order $2k + 1$ (if integer) is null for Δ_k . Taking advantage of this property may result in a fast version of the proposed algorithm.

However, calculation time problems are now less crucial than they used. The standard KS algorithm only takes 0.36 s¹ to process the entire data set of Fig. 1, so real time computations can probably be achieved.

VI. HYPERPARAMETERS ESTIMATION

The estimated \mathbf{a}_m -sequence and spectra sequence depends on $M + 4$ hyperparameters: smoothness and AR orders k and P , power sequence r_m^ε , and two regularization parameters λ_s and λ_d .

A. Power Parameters

The M parameters r_m^ε are needed by the proposed RegLS method as well as the LS and ALS procedures, and the same empirical estimates will be used for all of them. In the criterion (10), parameters r_m^ε only act as weighting coefficients, so that the successive terms are of equivalent weight. The proposed empirical technique replaces the prediction error powers r_m^ε by the signal powers r_m themselves. A simple empirical estimate $\hat{r}_m = \mathbf{y}_m^\dagger \mathbf{y}_m / N$ could be used. However, since the estimation variance is high for $N = 8$, in practice, a more efficient technique consists in smoothing the sequence \hat{r}_m . Let us note that [2] proposes a scheme, which is equivalent in principle.

B. Order Parameters

The proposed framework allows us to estimate long AR models to describe various spectral shapes. Moreover, by choosing the maximal order $P = N - 1$, we get rid of the difficult problem of model-order selection. In fact, as expected and confirmed in Section VII-C, as long as P is large enough, it does not significantly affect the spectral shape.

On the other hand, to our experience, the smoothness order k does not affect the spectrum sequence provided that $k \neq 0$. So the smoothness order is *a priori* tuned to $k = 1$, i.e., a first-order derivative spectra penalization. Moreover, Section VII-C also provides a quantitative sensitivity study of the spectra sequence with regard to this parameter.

C. Regularization Parameters

The problem of regularization parameter estimation within the proposed framework is a delicate one. It has been extensively studied and several techniques have been proposed and compared [26], [31]–[35]. The ML approach is often chosen within the Bayesian framework mentioned in Remarks 2 and 3. The Gaussian likelihood function (1) and the Gaussian prior (9) together yield a Gaussian marginal law for the observed samples $f(\mathcal{Y}; \lambda_s, \lambda_d)$, i.e., the regularization parameter likelihood. The hyperparameter-co-log-likelihood (HCLL) is easily computed

¹The proposed algorithm has been implemented using the computing environment Matlab on a personal computer, Pentium III, with a 450 MHz CPU and 128 Mo of RAM.

for a given hyperparameter set, as a function of innovation vectors \mathbf{e}_m and covariances R_m , i.e., two of the KF subproducts

$$\text{HCLL}(\lambda_s, \lambda_d) = \sum_{m=1}^M \ln \det R_m + \mathbf{e}_m^\dagger R_m^{-1} \mathbf{e}_m$$

ignoring constant coefficients. This expression is the generalization of a more conventional identity, available for scalar observations [2]. The error covariance matrix R_m is an $L \times L$ matrix, L possibly ranging from $L = 1$ to $L = N + P$ according to the windowing form and model order. Since $L = 1$ is selected in the presented computations, no specific algorithm has been developed for inversion nor determinant calculations.

The ML estimate

$$\left(\hat{\lambda}_s^{\text{ML}}, \hat{\lambda}_d^{\text{ML}} \right) = \arg \min_{\lambda_s, \lambda_d} \text{HCLL}(\lambda_s, \lambda_d) \quad (31)$$

can be computed by means of several algorithms: coordinate/gradient descent algorithm [28] or EM algorithms [36], [37], but none of them can ensure global optimization. Here, the optimization stage is tackled by means of a coordinate descent algorithm with a golden section line search [28]. Since HCLL is a function of two variables only, the optimization stage only requires about 10 s.

VII. SIMULATION RESULTS AND COMPARISONS

The present section assesses the effectiveness of the proposed method, compared to the usual ones by processing the example shown in Fig. 1.

A. Quantitative Comparison Criterion

Since the true spectrum sequence is known in the presented simulations, quantitative criteria are computable on the basis of distances between estimated spectra $\hat{S}_m(\nu)$ and true ones $S_m(\nu)$, accumulated over the M bins. Normalized distances

$$L^r = \frac{\sum_{m=1}^M \int_0^1 |\hat{S}_m(\nu) - S_m(\nu)|^r d\nu}{\sum_{m=1}^M \int_0^1 |S_m(\nu)|^r d\nu}$$

with $r = 1$ and $r = 2$ have been computed. The normalization is chosen so that a null estimated spectrum results in a 100% error. Practically, the integrals are approximated by discrete summation over the frequency domain $\nu = q/Q$, $q \in \mathbb{N}_{Q-1}$, with $Q = 1024$.

B. Tuning Parameters

1) *Usual Methods*: Since no automatic parameter tuning is available for usual methods, these parameters have been chosen in order to produce the best L^2 distance. Moreover, we have checked that such a quantitative procedure finds itself in good agreement with the visual appreciation.

- 1) First of all, it is noticeable that, even for a short model, the nonwindowed and prewindowed methods systematically yield numerous spurious peaks. The best results

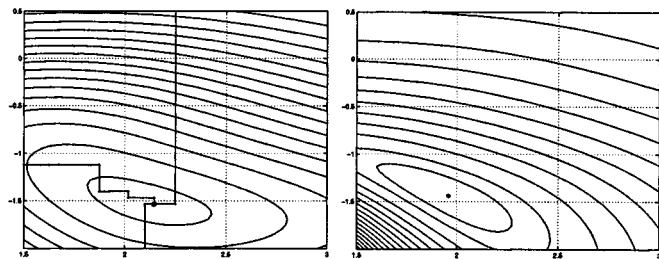


Fig. 2. The left and right figure, respectively, show HCLL and L^2 distance (L^1 behaves similarly) as a function of regularization parameters (λ_s, λ_d) , respectively [read on the vertical and the horizontal axis (\log_{10} scaled)]. In both cases, a star (*) locates the minimum.

have been obtained with the postwindowed form² (double-windowed behaves similarly) so, the estimated spectra are of poor resolution [15].

- 2) As expected, since the true spectra show up to three modes, the best results have been obtained with $P = 3$ for both LS and ALS.
- 3) Finally, as far as the ALS method is concerned, $W = 20$ has been selected.

2) *Regularized Method*: The HCLL function has been computed on a fine discrete \log_{10} grid of 100×100 values between -2 and 1 for λ_s and between 1 and 3 for λ_d . The result is the HCLL sheet shown in Fig. 2 (LHS). It is fairly regular and exhibits a single minimum at $\hat{\lambda}_s^{\text{ML}} = -1.53$ and $\hat{\lambda}_d^{\text{ML}} = 2.16$. Moreover, Fig. 2 right-hand side (RHS) shows the corresponding L^2 distances, and the strikingly similar behavior of $\text{HCLL}(\lambda_s, \lambda_d)$ and $L^2(\lambda_s, \lambda_d)$ is a strong argument in favor of the likelihood as a criterion for parameters tuning.

However, it must be mentioned that a variation of on-decade on λ_s or λ_d entails a nearly imperceptible variation in the estimated spectra and a fraction of percent error. This point is especially important for qualifying the robustness of the proposed method. Contrary to the choice of model order in the usual AR analysis, which is critical, the choice of (λ_s, λ_d) offers broad leeway and can be made reliably.

Practically, the adjustment is set using the coordinate descent algorithm, and Fig. 2 (LHS) illustrates its convergence from three different starting points.

C. Order Sensitivity

This section assesses the sensitivity of the method with regard to the order parameters k and P . For $P = 1$ to $P = 7$ and for $k = 0$ to $k = 2$ (step .25), we have computed the ML estimate (31)

$$\left(\hat{\lambda}_s^{\text{ML}}(P, k), \hat{\lambda}_d^{\text{ML}}(P, k) \right) = \arg \min_{\lambda_s, \lambda_d} \text{HCLL}(\lambda_s, \lambda_d, P, k)$$

and the corresponding optimal likelihood and distance

$$\text{HCLL}_{\text{opt}}(P, k) = \text{HCLL} \left(\hat{\lambda}_s^{\text{ML}}(P, k), \hat{\lambda}_d^{\text{ML}}(P, k), P, k \right)$$

²A possible explanation for this rather counterintuitive fact, is that the post-windowed form is somewhat “self penalizing,” i.e., the corresponding criterion incorporates quadratic penalization terms: $\mathbf{a}_m^\dagger M \mathbf{a}_m$, where M only depends upon the data.

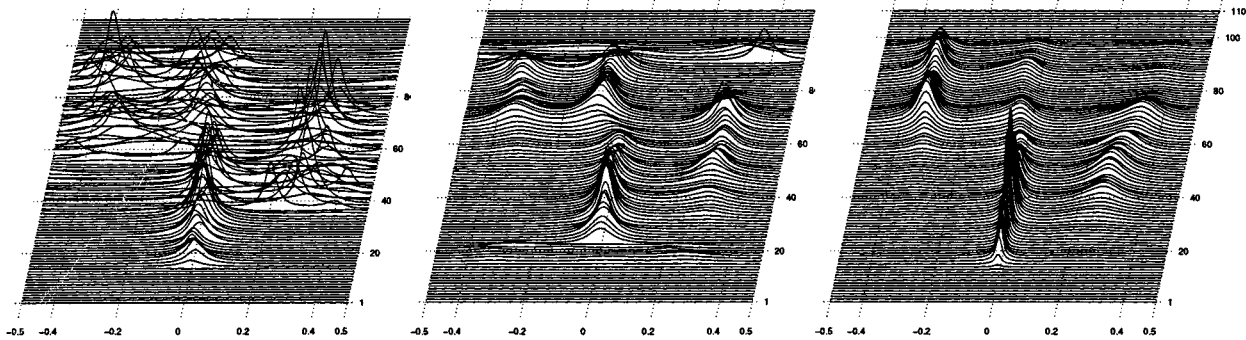


Fig. 3. (Top) Optimal likelihood $HCLL_{opt}(P, k)$ and (bottom) distances $L^2_{opt}(P, k)$ as a function of order P for several smoothness order $k = 0.5, 1, 1.5,$ and 2 .

$$L^r_{opt}(P, k) = L^r(\hat{\lambda}_s^{ML}(P, k), \hat{\lambda}_d^{ML}(P, k), P, k).$$

They are plotted in Fig. 3 as a function of P for the several values of k .

As far as the likelihood is concerned, the following applies.

- $HCLL_{opt}$ is a decreasing (almost linear) function of model order P : the ML selected order is the maximal one $P = N - 1 = 7$.
- $HCLL_{opt}$ does not depend on k (the four curves are over plotted) so that, given P , the triplet $(\lambda_s, \lambda_d, k)$ “over-parameterizes” the likelihood and k is indifferent.

As far as the L^2 is concerned, it still behaves similarly to the likelihood. It is roughly decreasing with P and not depending upon k . As a conclusion, the maximization of the likelihood with regard to k and P does not provide any improvement and the recommended scheme described in Section VI-B is an efficient one.

D. Qualitative Evaluation

We have then compared the usual methods at their best (optimally adjusted parameters knowing the true spectra) with the proposed method (automatic selection of regularization parameters without knowledge of the true spectra). The results obtained by LS, ALS, and RegLS are presented in Fig. 4. A simple qualitative comparison with the reference Fig. 1 already leads to four conclusions.

- 1) The ML strategy provides a good value for the regularization parameters, and the L^2 (and L^1) distance is in accordance with the qualitative assessment.
- 2) The effect of the regularization is obvious. Estimated spectra are in much greater conformity with the true ones. The spectrum shapes are reproduced more precisely in one, two, or three modes. Their positions and their amplitudes are correctly estimated.
- 3) Moreover, the spectral resolution for the ground clutter is strongly enhanced. It is essentially due to the coherent accounting for spectral and spatial continuity resulting in a robust nonwindowed form.
- 4) However, it can be seen that the sudden transitions at the beginning of the ground clutter is slightly oversmoothed. This can be expected from quadratic regularization and

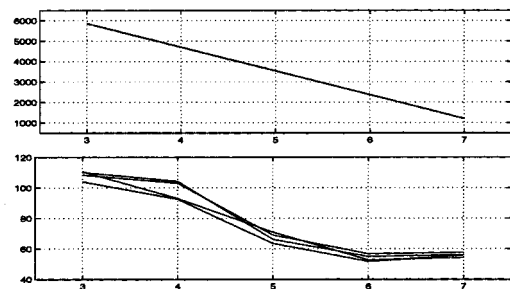


Fig. 4. Estimated spectra from left to right: usual LS estimate, adaptive LS estimate, and regularized LS estimate (proposed method). Corresponding true spectra and data are shown in Fig. 1. Quantitative results are given in Table I.

TABLE I
QUANTITATIVE COMPARISON OF THE PERIODOGRAM, LSMS, AND THE REGULARIZED ONE. L^1 AND L^2 INDICATES THE DISTANCES BETWEEN ESTIMATED AND TRUE SPECTRA

Method	L^2	L^1
Periodogram	87.1%	92.9%
Best LS	76.6%	85.4%
Best ALS	66.4%	75.5%
ML & RegLS	57.9%	69.2%

may be at least partially avoided by introducing non-quadratic regularization [38]–[40].

E. Quantitative Evaluation

In the nonadaptive context, quantitative comparisons have previously been performed in [1], [26]. The adaptive extension originally proposed by Kitagawa and Gersch has also been quantitatively assessed in [2].

For the proposed method, quantitative comparison have been achieved by evaluating L^1 and L^2 distances between true and estimated spectra. The results are listed in Table I and show an L^2 improvement of about 10% from periodogram to best LS, 10% from best LS to best ALS and 10% from best ALS to the entirely automatic proposed method.

VIII. CONCLUSION AND PERSPECTIVES

This paper tackles short-time adaptive AR spectral estimation within the regularization framework. It proposes a new regular-

ized LS criterion accounting for spectral smoothness and spatial continuity. The criterion is efficiently optimized by a special Kalman smoother. In this sense, the present study significantly deepens the contributions of [1], [2], given that the latter separately address spectral smoothness and spatial continuity. Moreover, the proposed method is entirely unsupervised, and it is shown that ML regularization parameters are both formally achievable and practically useful. Finally, a simulated comparison study is proposed in the field of Doppler radars. It shows an improvement of about 10%, comparing some usual methods at their best versus the entirely automatic proposed one.

Future works will be devoted to compensate for the over-smoothing character of quadratic regularization in the presence of spatial breaks. [41] accounts for spatial continuity while preserving breaks by way of a non-Gaussian state model and extended KF algorithms. In our mind, a preferable approach could be to introduce nonquadratic convex penalty terms and to minimize the resulting criterion using descent algorithms [38], [39], [42].

ACKNOWLEDGMENT

The authors wish to thank Mr. Grün and Mrs. Groen for their expert editorial assistance.

REFERENCES

- [1] G. Kitagawa and W. Gersch, "A smoothness priors long AR model method for spectral estimation," *IEEE Trans. Automat. Contr.*, vol. AC-30, pp. 57–65, Jan. 1985.
- [2] ———, "A smoothness priors time-varying AR coefficient modeling of nonstationary covariance time series," *IEEE Trans. Automat. Contr.*, vol. AC-30, pp. 48–56, Jan. 1985.
- [3] Y. Grenier, "Modèles ARMA à coefficients dépendant du temps," *Trait. Signal*, vol. 3, no. 4, pp. 219–233, 1986.
- [4] R. Kuc, "Employing spectral estimation procedures for characterizing diffuse liver disease," in *Tissue Characterization with Ultrasound*, 1986, ch. 6, pp. 147–166.
- [5] J. Idier, J.-F. Giovannelli, and B. Querleux, "Bayesian time-varying AR spectral estimation for ultrasound attenuation measurement in biological tissues," in *Proc. Section Bayesian Statistical Science*, Alicante, Spain, 1994, pp. 256–261.
- [6] P. Péronneau, *Vélocimétrie Doppler. Application en Pharmacologie Cardiovasculaire Animale et Clinique*. Paris, France: INSERM, 1991.
- [7] D. K. Barton and S. Leonov, *Radar Technology Encyclopedia*. London, U.K.: Artech House, 1997.
- [8] G. Le Foll, P. Larzabal, and H. Clergeot, "A new parametric approach for wind profiling with Doppler radar," *Radio Sci.*, vol. 32, pp. 1391–1408, July–Aug. 1997.
- [9] J. M. B. Dias and J. M. N. Leitão, "Nonparametric estimation of mean Doppler and spectral width," *IEEE Trans. Geosci. Remote Sensing*, vol. 38, pp. 271–282, Jan. 2000.
- [10] N. Allan, C. L. Trumpf, D. B. Trizna, and D. J. McLaughlin, "Dual-polarized Doppler radar measurements of oceanic fronts," *IEEE Trans. Geosci. Remote Sensing*, vol. 37, pp. 395–417, Jan. 1999.
- [11] F. Barbaresco, "Turbulences estimation with new regularized super-resolution Doppler spectrum parameters," in *RADME* Rome, Italy, 1998.
- [12] M. Basseville, N. Martin, and P. Flandrin, "Méthodes temps-fréquence et segmentation de signaux," in *Numéro Spécial de Traitement du Signal*. Paris, France: JOUVE, 1992, vol. 9.
- [13] J. B. Allen, "Short term spectral analysis, synthesis, and modification by discrete Fourier transform," *IEEE Trans. Acoust., Speech, Signal Processing*, vol. ASSP-25, pp. 235–238, June 1977.
- [14] J. B. Allen and L. R. Rabiner, "A unified approach to short-time Fourier analysis and synthesis," *Proc. IEEE*, vol. 65, pp. 1558–1564, Nov. 1977.

- [15] S. L. Marple, *Digital Spectral Analysis With Applications*. Englewood Cliffs, NJ: Prentice-Hall, 1987.
- [16] S. M. Kay, *Modern Spectral Estimation*. Englewood Cliffs, NJ: Prentice-Hall, 1988.
- [17] B. Picinbono, *Éléments de Probabilité*. Gif-sur-Yvette, France: Cours de SUPÉLEC, 1991, vol. 1127.
- [18] S. M. Kay, "Recursive maximum likelihood estimation of autoregressive processes," *IEEE Trans. Acoust., Speech, Signal Processing*, vol. ASSP-21, pp. 56–65, 1983.
- [19] D. T. Pham, "Maximum likelihood estimation of the autoregressive model by relaxation on the reflection coefficients," *IEEE Trans. Signal Processing*, vol. 36, pp. 1363–1367, Aug. 1988.
- [20] S. M. Kay and S. L. Marple, "Spectrum analysis—A modern perspective," *Proc. IEEE*, vol. 69, pp. 1380–1419, Nov. 1981.
- [21] H. Akaike, "Statistical predictor identification," *Ann. Inst. Statist. Math.*, vol. 22, pp. 207–217, 1970.
- [22] ———, "A new look at the statistical model identification," *IEEE Trans. Automat. Contr.*, vol. AC-19, pp. 716–723, Dec. 1974.
- [23] E. Parzen, "Some recent advances in time series modeling," *IEEE Trans. Automat. Contr.*, vol. AC-19, pp. 723–730, Dec. 1974.
- [24] J. Rissanen, "Modeling by shortest data description," *Automatica*, vol. 14, pp. 465–471, 1978.
- [25] T. J. Ulrych and R. W. Clayton, "Time series modeling and maximum entropy," *Phys. Earth Planetary Interiors*, vol. 12, pp. 188–200, 1976.
- [26] J.-F. Giovannelli, G. Demoment, and A. Herment, "A Bayesian method for long AR spectral estimation: A comparative study," *IEEE Trans. Ultrason. Ferroelect. Freq. Contr.*, vol. 43, pp. 220–233, Mar. 1996.
- [27] A. Houacine and G. Demoment, "A Bayesian method for adaptive spectrum estimation using high order autoregressive models," in *Mathematics in Signal Processing II*, J. G. McWhirter, Ed. Oxford, U.K.: Clarendon, 1990, pp. 311–323.
- [28] D. P. Bertsekas, *Nonlinear Programming*. Belmont, MA: Athena Scientific, 1995.
- [29] A. H. Jazwinski, *Stochastic Process and Filtering Theory*. New York: Academic, 1970.
- [30] A. H. Sayed and T. Kailath, "A state-space approach to adaptive RLS filtering," *IEEE Trans. Signal Processing Mag.*, pp. 18–60, July 1994.
- [31] G. H. Golub, M. Heath, and G. Wahba, "Generalized cross-validation as a method for choosing a good ridge parameter," *Technometrics*, vol. 21, pp. 215–223, May 1979.
- [32] D. M. Titterton, "Common structure of smoothing techniques in statistics," *Int. Statist. Rev.*, vol. 53, no. 2, pp. 141–170, 1985.
- [33] P. Hall and D. M. Titterton, "Common structure of techniques for choosing smoothing parameter in regression problems," *J. R. Statist. Soc. B*, vol. 49, no. 2, pp. 184–198, 1987.
- [34] A. Thompson, J. C. Brown, J. W. Kay, and D. M. Titterton, "A study of methods of choosing the smoothing parameter in image restoration by regularization," *IEEE Trans. Pattern Anal. Machine Intell.*, vol. 13, pp. 326–339, Apr. 1991.
- [35] N. Fortier, G. Demoment, and Y. Goussard, "GCV and ML methods of determining parameters in image restoration by regularization: Fast computation in the spatial domain and experimental comparison," *J. Visual Comm. Image Repres.*, vol. 4, pp. 157–170, June 1993.
- [36] R. Shumway and D. Stoffer, "An approach to time series smoothing and forecasting using the EM algorithm," *J. Time Series Anal.*, pp. 253–264, 1982.
- [37] S. E. Levinson, L. R. Rabiner, and M. M. Sondhi, "An introduction to the application of the theory of probabilistic function of a Markov process to automatic speech processing," *Bell Syst. Tech. J.*, vol. 62, pp. 1035–1074, Apr. 1982.
- [38] C. A. Bouman and K. D. Sauer, "A generalized Gaussian image model for edge-preserving MAP estimation," *IEEE Trans. Image Processing*, vol. 2, pp. 296–310, July 1993.
- [39] P. J. Green, "Bayesian reconstructions from emission tomography data using a modified EM algorithm," *IEEE Trans. Med. Imag.*, vol. 9, pp. 84–93, Mar. 1990.
- [40] L. Rudin, S. Osher, and C. Fatemi, "Nonlinear total variation based noise removal algorithm," *Phys. D*, vol. 60, pp. 259–268, 1992.
- [41] G. Kitagawa, "Non-Gaussian state-space modeling of nonstationary time series," *J. Amer. Statist. Assoc.*, vol. 82, pp. 1032–1041, Dec. 1987.
- [42] J. Idier, "Convex half-quadratic criteria and interacting auxiliary variables for image restoration," *IEEE Trans. Image Processing*, vol. 10, July 2001.



Jean-François Giovannelli was born in Béziers, France, in 1966. He received the degree from the École Nationale Supérieure de l'Électronique et de ses Applications, Paris, France, and the Ph.D. degree in physics from the Laboratoire des Signaux et Systèmes, Université de Paris-Sud, Orsay, France, in 1990 and 1995, respectively.

He is currently an Assistant Professor with the Département de Physique, Université de Paris-Sud, Paris, France. He is interested in regularization methods for inverse problems in signal and image processing, mainly in spectral characterization. Application fields essentially concern radar and medical imaging.



Daniel Muller was born in Saint-Cloud, France, on August 12, 1961. He received the degree from "Ecole Polytechnique," Palaiseau, France, in 1983, and the Ph.D. degree in electrical engineering from "Ecole Supérieure d'Electricité," Gif-sur-Yvette, France, in 1985.

In 1985, he joined Thales, formerly Thomson-CSF, France, where he was involved in the functional design and performance assessment of several new Radar products and demonstrators. He is now in charge of the Algorithms and Functional Architecture Department, in the Technical Direction of the "Radar Development" Business Unit, Thales Air Defence.



Jérôme Idier was born in France in 1966. He received the diploma degree in electrical engineering from the École Supérieure d'Électricité, Paris, France, and the Ph.D. degree in physics from the Université de Paris-sud, Orsay, in 1988 and 1991, respectively.

Since 1991, he has been with the Centre National de la Recherche Scientifique, Paris, France, assigned to the Laboratoire des Signaux et Systèmes. His major scientific interests are in probabilistic approaches to inverse problems for signal and image processing.



Guy Desodt was born in Bailleul, France, on May 8, 1952.

He has been with the Thales Group, formerly Thomson-CSF, France, for 22 years, working in the area of ground-based and naval radars. His main areas of interest are innovative radar architectures, including new signal and data processing chains, like adaptive Doppler processing, multibeam adaptive digital beam forming, and noncooperative target recognition.